Journal of Alloys and Compounds 509 (2011) 5662–5666

Contents lists available at ScienceDirect

Journal of Alloys and Compounds

journal homepage: www.elsevier.com/locate/jallcom

Synthesis of $LiFePO_4$/C cathode materials through an ultrasonic-assisted rheological phase method

Hyun-Ju Kim[a], Jeong-Min Kim[a], Woo-Seong Kim[b], Hoe-Jin Koo[c], Dong-Sik Bae[d], Hyun-Soo Kim[a,*]

[a] *Korea Electrotechnology Research Institute, Changwon 641-120, Republic of Korea*
[b] *Daejung EM Co., Incheon 429-450, Republic of Korea*
[c] *Battery R&D Association of Korea, Seoul 137-894, Republic of Korea*
[d] *Changwon National University, Changwon 641-773, Republic of Korea*

ARTICLE INFO

Article history:
Received 27 January 2011
Received in revised form 18 February 2011
Accepted 22 February 2011
Available online 26 February 2011

Keywords:
Lithium-ion battery
$LiFePO_4$
Cathode active material
Rheological phase method
Polyvinyl butyral (PVB)

ABSTRACT

$LiFePO_4$/C active material was synthesized using an ultrasonic-assisted rheological phase method. In addition, polyvinyl butyral (PVB) was added in various concentrations to provide carbon coating on the surface of the $LiFePO_4$ particles for enhanced electrical conductivity. The crystal structure, morphology, and carbon coating layer of the synthesized $LiFePO_4$/C was analyzed using X-ray diffraction (XRD), scanning electron microscopy (SEM), and transmission electron microscopy (TEM), respectively. The electrochemical performance of $LiFePO_4$/C, such as initial capacity, rate capability, cycling performance and EIS, were also evaluated. The synthesized particle had a size range of 100–150 nm and a carbon layer of about 8 nm. The $LiFePO_4$/C (5 wt% PVB) delivered an initial discharge capacity of 167.5 mAh/g at a 0.1 C rate. It also showed an excellent capacity retention ratio of 100% after the 50th charging/discharging. EIS results demonstrate that the charge transfer resistance of the sample decreases greatly by coating with 5 wt% PVB.

1. Introduction

Lithium iron phosphate ($LiFePO_4$) is a promising cathode material for lithium rechargeable batteries. This material has many advantages compared to conventional cathode materials such as $LiCoO_2$, $LiNiO_2$ and $LiMn_2O_4$; it is environmentally benign, inexpensive, and thermally stable in the fully charged state [1,2]. Excellent thermal safety, due to the strong covalent bond properties of PO_4, makes $LiFePO_4$ highly suitable for electric vehicles (EV) [3,4].

However, compared to the conductivity of $LiCoO_2$ (10^{-2} to 10^{-3} S/cm), $LiFePO_4$ has both a low conductivity (10^{-9} to 10^{-10} S/cm) and diffusion coefficient of lithium-ion (1.8×10^{-14} cm^2/S) [5,6]. Utilizing carbon-coating [7–12] and smaller particle sizes [13–18] have been attempted to overcome these drawbacks in using $LiFePO_4$ because a smaller $LiFePO_4$ particle size could shorten the diffusion length of the Li-ion, while carbon-coating would increase surface electronic conductivity. In addition to the traditional solid-state reaction synthesis routine, alternative synthesis processes including sol–gel, hydrothermal, co-precipitation, microwave heating, etc., have been continually developed [19–22]. However, mass production is difficult with these methods because of the complicated synthesis techniques required and the difficulty in controlling them.

This study reports on $LiFePO_4$/C synthesized by an ultrasonic-assisted rheological phase method. In a rheological phase system, the solid powders and liquid substances are uniformly distributed so the surface area of the solid particles can be utilized more efficiently than in the solid state phase due to the close contact between the solid and liquid sections. It is also convenient for heat exchange and should ease the diffusion of lithium into the material [23]. PVB (polyvinylbutyral) solution was used as a carbon source to produce *in situ* carbon to improve the electronic conductivity of $LiFePO_4$. In addition, using an ultrasonic process could make the solid powders to disperse more uniformly in liquid substances, and to some extent effectively restrain the agglomeration of solid powders. Therefore, it can be expected that this ultrasonic-assisted rheological phase method can be employed to synthesize nano-sized $LiFePO_4$/C with a homogeneous particle size to improve the electrochemical performance of $LiFePO_4$.

The crystal structure, morphology, and carbon coating layer of the synthesized $LiFePO_4$/C were analyzed using X-ray diffraction (XRD), scanning electron microscopy (SEM), and transmission electron microscopy (TEM), respectively. The electrochemical performance of $LiFePO_4$/C, such as initial capacity, rate capability, cycling performance and EIS were also evaluated.

2. Experimental

As shown in Fig. 1, Fe oxalate (Junsei), Li hydroxide (Sigma–Aldrich) and ammonium dihydrogen phosphate (Sigma–Aldrich) were used as the starting materials for synthesizing $LiFePO_4$. The weight ratios of 1:20 of the initial material and zirconia

---

* Corresponding author. Tel.: +82 55 280 1660; fax: +82 55 280 1590.
E-mail address: hskim@keri.re.kr (H.-S. Kim).

0925-8388/$ – see front matter © 2011 Elsevier B.V. All rights reserved.
doi:10.1016/j.jallcom.2011.02.113

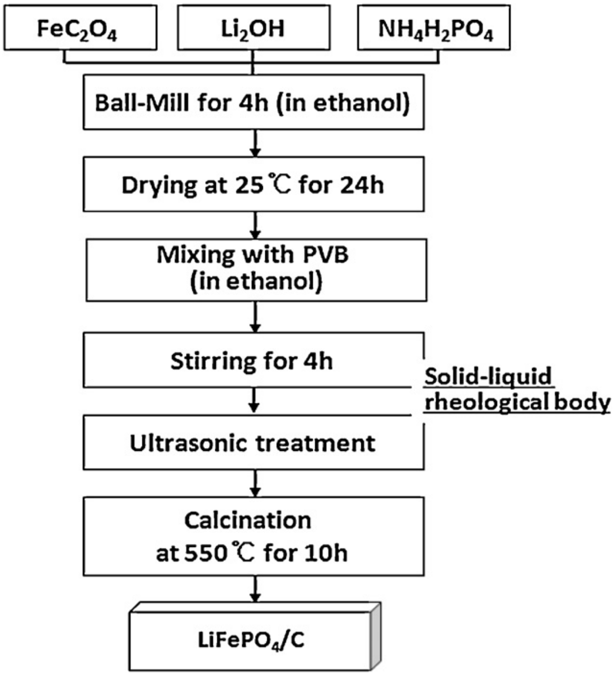

Fig. 1. Synthesis of carbon-coated $LiFePO_4$/C powder through an ultrasonic-assisted rheological phase method.

balls, was inserted into ethanol media and synthesized in the ball-mill for 4 h at 500 rpm. The synthesized material was dried at 25 °C for 24 h to remove foreign matter. Then the milled powders were mixed with dissolved polyvinylbutyral(PVB) in ethanol media to obtain a mixture in a solid–liquid rheological state. The solid–liquid rheological state mixture was continuously stirred for 4 h. Subsequently, ultrasonication was conducted at 50 °C for 1 h to homogenize the $LiFePO_4$/C particles. This was dried at 80 °C for 6 h in an argon gas atmosphere to adequately eliminate the ethanol. Then the sample was heat-treated at 550 °C for 10 h in an argon gas atmosphere to acquire the $LiFePO_4$/C synthesized material. During the heat treatment, PVB was converted into carbon, and a coating layer was formed on the surface of the active material.

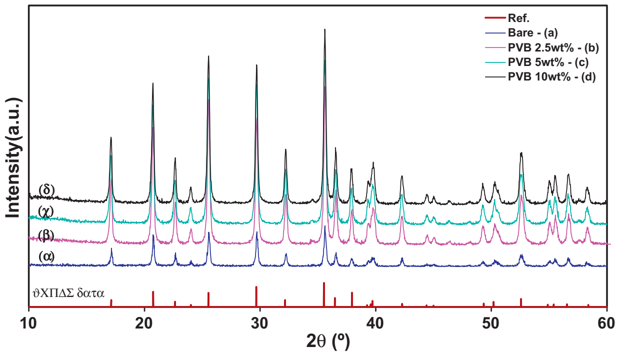

Fig. 2. XRD patterns of $LiFePO_4$ and $LiFePO_4$/C composite with different carbon source content. (JCPDS 40-1499).

X-ray diffraction analysis was performed to observe the crystal structure and any impurities in the synthesized active material, using an X-pert PW3830 (Philips Co.). The Cu Kα line was used under conditions of 40 kV and 30 mA, with a scan speed of 0.04°/s and a scan range of 10–60° (2θ). In addition, field emission SEM (FE-SEM, S-4800, Hitachi Co.) analysis was conducted to measure the particle size and surface morphology. Before observation, Os (Osmium) was coated on the surface of the specimen to enhance electrical conductivity. The magnifications used were 30,000×. The morphology of the carbon coating on the particles was confirmed by using FE-TEM (JEM2100F, JEOL Co.).

To examine the electrochemical performance of the synthesized active materials, the active material ($LiFePO_4$/C), a conducting agent (Super-P Black), and a binder, polyvinylidene fluoride (PVDF), were distributed into an n-methyl pyrrolidone (NMP) solvent at a ratio of 75:15:10 (wt%) to obtain a slurry. The slurry was then coated onto aluminum foil and dried for 12 h at a temperature of 100 °C. Pressing followed, using a hot-roll press, at the temperature of 110 °C. A lithium anode, a separator (Celguard 3501), and the thus-produced cathode electrode were laminated for assembly into coin cells (CR2032 type). EC (ethylene carbonate)/DEC (dimethyl ethyl carbonate) = 1/1 (vol.%) with dissolved $LiPF_6$ was used as the electrolyte.

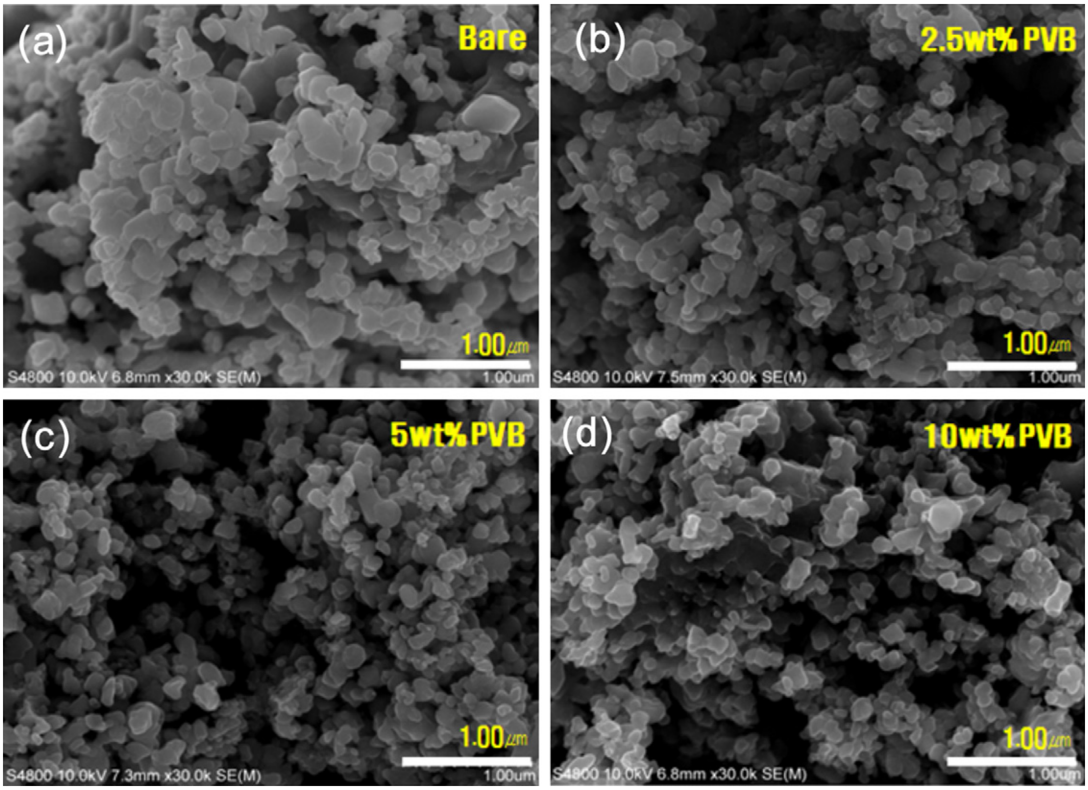

Fig. 3. FE-SEM images of $LiFePO_4$ (a) and $LiFePO_4$/C (b), (d) composite with different carbon source content.

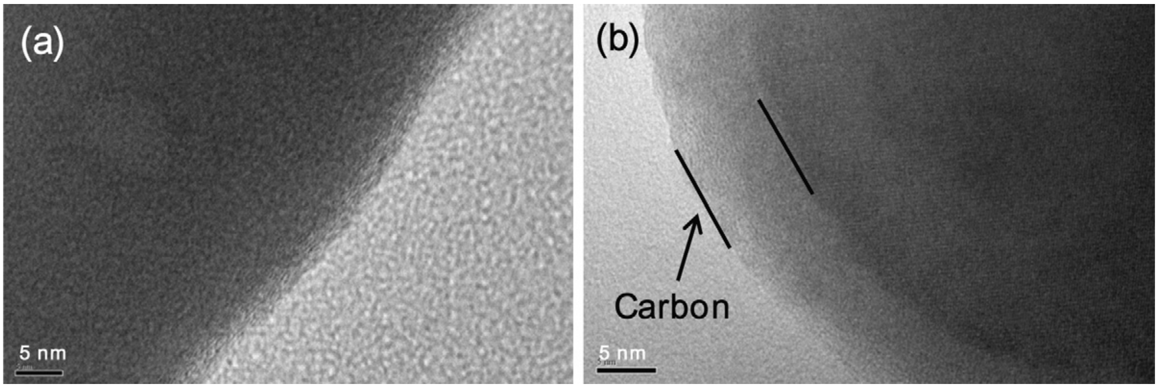

Fig. 4. FE-TEM images of $LiFePO_4$ (a) and $LiFePO_4/C$ (b) composite with 5 wt% carbon source.

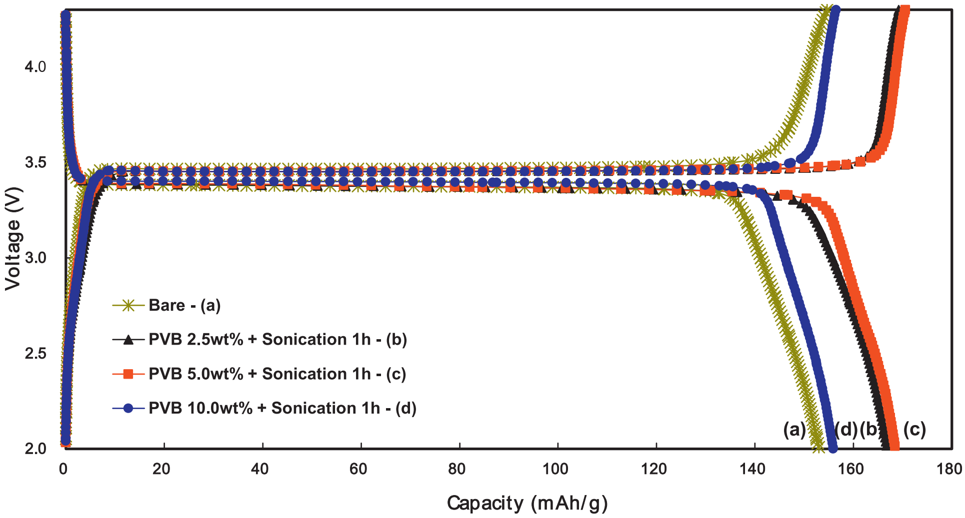

Fig. 5. Initial charge–discharge curves of $LiFePO_4/C$ with different carbon source content.

The electrochemical performances of the synthesized $LiFePO_4/C$ cathode materials were measured using a battery cycler (TOCAT-3100, TOYO System). The materials were charged and discharged over a voltage range of 2.0–4.3 V by CC (constant current)–CV (constant voltage) method. Rate capability was evaluated at current rates of 0.1, 0.2, 0.5, 1.0, 3.0, 5.0, 10 and 20 C. The cycling performance of the synthesized $LiFePO_4/C$ material was also tested at a current rate of 0.5C.

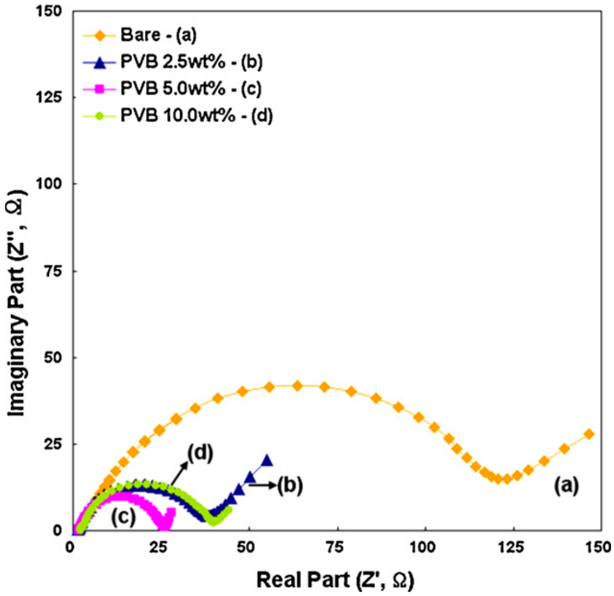

Fig. 6. EIS (Nyquist plots) of the bare $LiFePO_4$ and $LiFePO_4/C$ composite with different carbon source content after one cycle.

EIS was analyzed for the discharged cell using an IM6 (ZAHNER, Germany). The frequency range was measured in 1 Hz–1 MHz, and amplitude was measured in 10 mV.

3. Results and discussion

Fig. 2 shows XRD patterns of the $LiFePO_4$ and $LiFePO_4/C$ synthesized powders with different carbon source contents. All peaks can be indexed as pure and well-crystallized $LiFePO_4$ phase with an ordered olivine structure and a space group of *Pnma* (JCPDS card no. 40-1499). Carbon itself prevents the oxidation of Fe^{2+} to Fe^{3+}, which hinders the appearance of impurity, and to stop the growth of the $LiFePO_4$ particle [24].

Fig. 3 shows the surface morphology of the as-synthesized $LiFePO_4$ (Fig. 3(a)) and $LiFePO_4/C$ (Fig. 3(b) and (d)) composite with different carbon source content, observed with FE-SEM. The $LiFePO_4$ had an irregular primary particle and was agglomerated. However, the $LiFePO_4/C$ powder consisted of small particles in the range of 100–150 nm and size distribution was uniform. Compared to the traditional solid-state reaction route [25,26], or even the solution method [27,28], the particle size obtained by the present rheological phase method is much smaller and the size distribution uniform. As a powder with such small particles has a large specific surface area, the conclusion was drawn that this suitability for the convenient movement of lithium ions should enhance electrochemical performance.

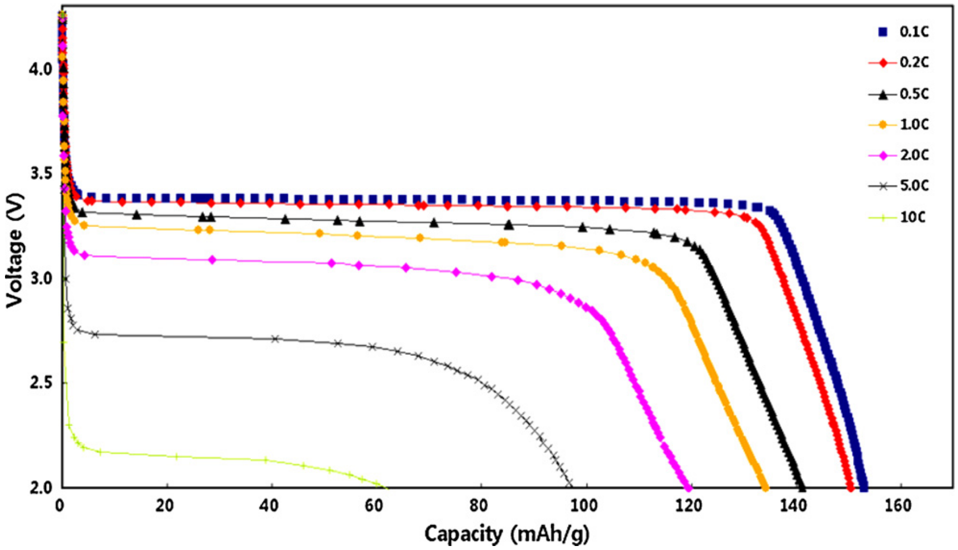

Fig. 7. Charge–discharge curves of $LiFePO_4$ (Bare) at various current rates.

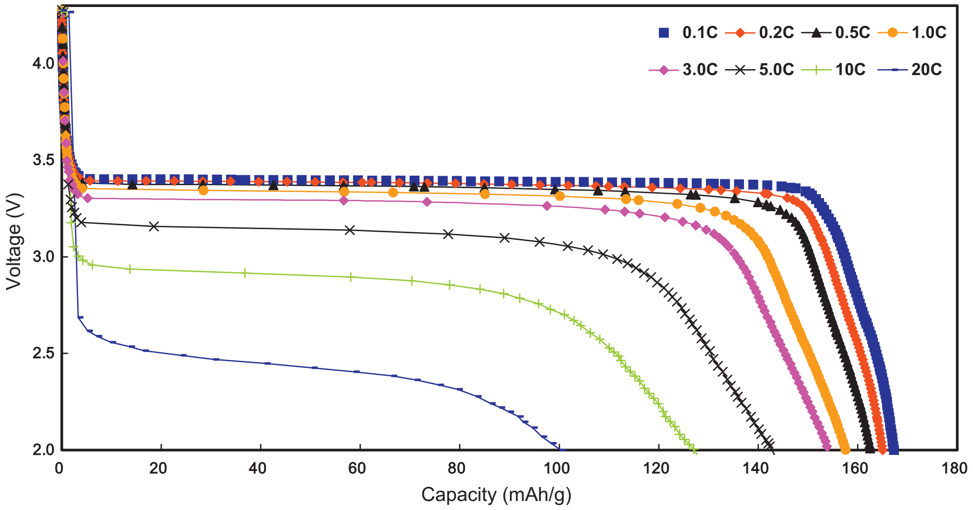

Fig. 8. Charge–discharge curves of $LiFePO_4$/C at various current rates. (PVB 5.0 wt%).

Fig. 4 shows an FE-TEM image of the $LiFePO_4$ (Fig. 4(a)) and $LiFePO_4$/C (PVB = 5.0 wt%) powder (Fig. 4(b)). A comparative look at the images clearly depicts the presence of carbon coverage over the grains. The carbon layer gained through heat treatment formed a homogeneous coating of approximately 5–10 nm in thickness. Such a carbon layer lowers the interface resistance and performs the role of limiting particle growth during the heat treatment process. As a result, this process allows for the convenient diffusion of lithium-ions, and improvement of electrochemical performance can be expected.

Fig. 5 shows the first cycle charge and discharge characteristics of the $LiFePO_4$ and $LiFePO_4$/C with different carbon source content synthesized by an ultrasonic-assisted rheological phase method. The $LiFePO_4$/C synthesized with ultrasonic treatment for

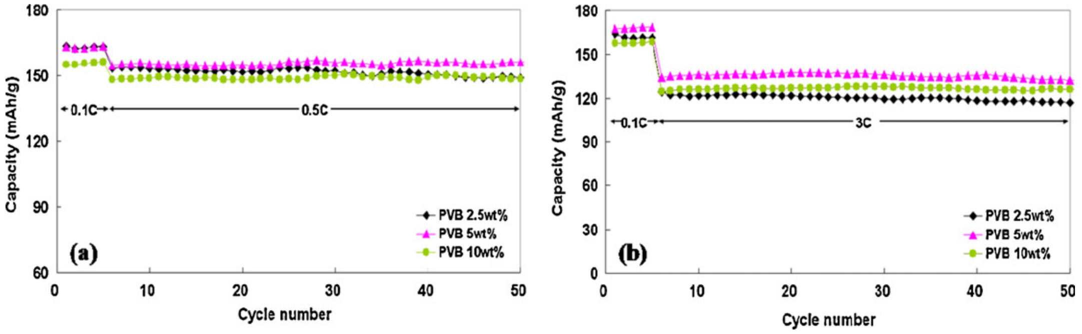

Fig. 9. Cycle performances of $LiFePO_4$ and $LiFePO_4$/C with different carbon source content at (a) 0.5 C and (b) 3.0 C rates at room temperature.

1 h showed the best electrochemical properties. The capacity of the material decreased as the ultrasonic time lengthened. It is believed that the capacity decrease was brought about by the oxidation of Fe(II) because the longer sonication increases the temperature by adding more energy. Accordingly, the active material was synthesized by fixing the sonication time for 1 h. As shown in Fig. 5, the appearance of well-defined voltage plateaus at approximately 3.5 and 3.4 V on the charge and discharge curves reflect the typical characteristics of olivine $LiFePO_4$. The pristine $LiFePO_4$ delivered the lowest discharge capacity of 153.0 mAh/g, while the initial capacity of the $LiFePO_4/C$ material was 166.2, 167.5, 155.9 mAh/g as the amount of carbon source on the active material increased from 2.5 to 10.0 wt%. Notably, excellent initial discharging capacity very close to the theoretical capacity was shown with 5 wt% PVB as a carbon source.

EIS was applied to further analyze the effect of PVB coating on electrode impedance. Before EIS tests, all the half-cells were discharged after charging in a 0.1C. Fig. 6 represents the Nyquist plots of $LiFePO_4$ and $LiFePO_4/C$ composite at ambient temperature. The Nyquist plots of all samples combine an intercept at high frequency, followed by a semicircle in the middle-high frequency region and a straight line in the low frequency region. An intercept at the Z_{re} axis at a high frequency corresponded to the ohmic resistance (R_e), which represented the resistance of the electrolyte and electrode. The semicircle in the middle frequency range indicated the charge transfer resistance (R_{ct}). The inclined line in the low frequency range represented the Warburg impedance (Z_w), which was associated with lithium-ion diffusion in $LiFePO_4$ particles [29]. In the middle-high frequency region, after carbon-coated $LiFePO_4/C$, the sample exhibited a smaller charge-transfer resistance (below 40 Ω) than that of the carbon un-coated $LiFePO_4$ (120 Ω). The charge-transfer resistance was the lowest in 25 Ω for the case of 5.0 wt% PVB. The lower R_{ct} value of the sample with carbon-coated $LiFePO_4/C$ indicates a lower electrochemical polarization, which can be attributed to the smaller particles. Smaller particle size is associated with lower electronic and/or ionic resistance at the boundary of the crystallites within each polycrystalline particle of the active material, thus improving the reversible capacity of $LiFePO_4/C$ materials [30].

Fig. 7 shows the rate capability of pristine $LiFePO_4$. As shown in figure, the discharge capacity of the $LiFePO_4$ powder was 153.0, 150.5, 141.3, 134.3, 119.4, 97.4, 62.3 mAh/g at the 0.1, 0.2, 0.5, 1.0, 3.0, 5.0 and 10.0 C rate. The $LiFePO_4$ powder showed an excellent discharging capacity of 153.0 mAh/g at 0.1 C. It is thought that the active material was coated with a small quantity of carbon in the Fe oxalate (FeC_2O_4) precursor and eventually contributed to improvement in electric conductivity.

Fig. 8 shows the rate capability performance of the synthesized $LiFePO_4/C$ (5 wt% PVB) material. As shown in figure, the discharge capacity of the $LiFePO_4/C$ powder was 167.5, 165.0, 162.6, 157.6, 154.2, 143.2 mAh/g at the 0.1, 0.2, 0.5, 1.0, 3.0, and 5.0 C rate, respectively. The material delivered a discharge capacity of 127.0 mAh/g at the high discharge current rate of 10.0 C, which indicated an outstanding capacity retention ratio of 75.9% against the 0.1 C rate. As a result, electrical conductivity is improved due to the carbon coating, and the diffusion of lithium ions occurred smoothly due to the optimized particle size and shape because crystallization was created without impurities.

Fig. 9 shows the cycling performance of $LiFePO_4/C$ with different carbon source contents. Cycling began with five charging/discharging formations at 0.1 C, executed 50 times. The initial discharge capacity of $LiFePO_4/C$ (5 wt% PVB) at 0.5 C rate was 154.6 mAh/g, and after 50 cycles, 156.3 mAh/g, which demonstrates a 100% capacity retention rate. Also, initial discharge capacity of $LiFePO_4/C$ (5 wt% PVB) at 3 C rate was 133.9 mAh/g, and after 50 cycles, 132.3 mAh/g, which demonstrates a 98.8% capacity retention rate.

4. Summary

$LiFePO_4/C$ active material was synthesized using an ultrasonic-assisted rheological phase method. No impurities such as Fe^{3+} or Li_3PO_4 could be seen in the synthesized active material. About 100–150 nm particle sizes were observed from FE-SEM analysis. HR-TEM analysis shows that the carbon coating layers were uniformly distributed on particle surfaces. The $LiFePO_4/C$ (5 wt% PVB) delivered an initial discharge capacity of 167.5 mAh/g at 0.1 C rate. It also showed an excellent capacity retention ratio of 100% after the 50th charging/discharging. EIS results demonstrate that the charge transfer resistance of the sample decreases greatly by applying a coating amount of 5 wt% PVB. By carbon coating $LiFePO_4$, electrical conductivity could be improved, irreversible capacity could be reduced, and hence lithium could be diffused smoothly, thereby increasing discharge capacity and cycleability.

Acknowledgements

This research was supported by a grant (code #: 2010K000328) from 'Center for Nanostructured Materials Technology' under '21st Century Frontier R&D Programs' of the Ministry of Education, Science and Technology, Korea.

References

[1] A.S. Anderson, J.O. Thomas, J. Power Sources 97–98 (2001) 498.
[2] N. Ravet, M. Gauthier, K. Zaghib, J.B. Goodenough, A. Mauger, F. Gendron, C.M. Julien, J. Chem. Mater. 19 (2007) 2595.
[3] K. Zaghib, P. Charest, A. Guerfi, J. Shim, M. Perrier, K. Striebel, J. Power Sources 146 (2005) 380.
[4] S. Beninati, L. Damen, M. Mastragostino, J. Power Sources 180 (2008) 875.
[5] D. Zane, M. Carewska, S. Scaccia, F. Cardellini, P.P. Prosini, Electrochem. Acta 49 (2004) 4259.
[6] G. Arnold, J. Garche, R. Hemmer, S. Ströbele, C. Vogler, M. Wohlfahrt-Mehrens, J. Power Sources 119 (2003) 247.
[7] H. Huang, S.-C. Yin, L.F. Nazar, Electrochem. Solid-State Lett. 4 (2001) A170.
[8] H.S. Kim, B.W. Cho, W.I. Cho, J. Power Sources 132 (2004) 235.
[9] R. Dominko, J.M. Goupil, M. Bele, M. Gaberseek, M. Remskar, D. Hanzel, J. Jamnik, J. Electrochem. Soc. 152 (2005) A843.
[10] B.F. Wang, Y.L. Qiu, L. Yang, Electrochem. Commun. 8 (2006) 1801.
[11] G.T.-K. Fey, T.-L. Lu, J. Power Sources 178 (2008) 807.
[12] M. Maccario, L. Croguennec, F. Le Cras, C. Kelmas, J. Power Sources 183 (2008) 411.
[13] A. Yamada, S.C. Chung, K. Hinokuma, J. Electrochem. Soc. 148 (2001) A224.
[14] M. Piana, B.L. Cushing, J.B. Goodenough, N. Penazzi, Solid State Ionics 175 (2004) 233.
[15] G. Meligrana, C. Gerbaldi, A. Tuel, S. Bodoardo, N. Penazzi, J. Power Sources 160 (2006) 516.
[16] D. Choi, P.N. Kumta, J. Power Sources 163 (2007) 1064.
[17] S.B. Lee, S.H. Cho, S.J. Cho, G.J. Park, S.H. Park, Y.S. Lee, Electrochem. Commun. 10 (2008) 1219.
[18] J.-C. Zheng, X.-H. Li, Z.-X. Wang, H.-J. Guo, S.-Y. Zhou, J. Power Sources 184 (2008) 574.
[19] F. Croce, A.D. Epifanio, J. Hassoun, A. Deptula, T. Olczac, B. Scrosati, Electrochem. Solid State Lett. 5 (2002) A47.
[20] S. Franger, F.L. Cras, C. Bourbon, H. Rouault, J. Power Sources 119–121 (2003) 252.
[21] K.S. Park, J.T. Son, H.T. Chung, S.J. Kim, C.H. Lee, H.G. Kim, Electrochem. Commun. 5 (2003) 839.
[22] S.F. Yang, P.Y. Zavalij, M.S. Whittingham, Electrochem. Commun. 3 (2001) 505.
[23] J. Xiao, H. Zhan, Y.H. Zhou, Mater. Lett. 58 (2004) 1620.
[24] C. Delacourt, P. Poizot, S. Levasseur, C. Masquelier, Electrochem. Solid-State Lett. 9 (2006) A325.
[25] K.S. Park, J.T. Son, H.T. Chung, S.J. Kim, C.H. Lee, K.T. Kang, H.G. Kim, Solid State Commun. 129 (2004) 311.
[26] Z. Chen, J.R. Dahn, J. Electrochem. Soc. 149 (2002) A1184.
[27] M.M. Doeff, Y. Hu, F. Mclarnon, R. Kostecki, Electrochem. Solid-State Lett. 6 (2003) A207.
[28] B.F. Wang, Y.Q.L. Yang, Electrochem. Commun. 8 (2006) 1801.
[29] X. Yin, K. Huang, S. Liu, J. Power Sources 195 (2010) 4311.
[30] Z.H. Xu, L. Xu, Q.Y. Lai, X.Y. Ji, Mater. Chem. Phys. 105 (2007) 80.